Investigating rockfall failure configurations using terrestrial laser scanner

Conference Paper · February 2014

CITATIONS
0

READS
80

4 authors, including:

Didier Hantz
Université Grenoble Alpes
72 PUBLICATIONS **1,004** CITATIONS

SEE PROFILE

Antoine Guerin
University of Lausanne
25 PUBLICATIONS **44** CITATIONS

SEE PROFILE

Michel Jaboyedoff
University of Lausanne
542 PUBLICATIONS **4,712** CITATIONS

SEE PROFILE

Investigating rockfall failure configurations using terrestrial laser scanner

Julie D'Amato[1], Didier Hantz[1], Antoine Guerin[2] & Michel Jaboyedoff[2]
[1] *Univ. Grenoble Alpes, ISTerre, F-38041 Grenoble, France; Julie.damato@ujf-grenoble.fr, +33 (0)476 63 51 63*
[2] *ISTE, University of Lausanne; Michel.Jaboyedoff@unil.ch, +41 (0)21 692 35 47*

Abstract

Terrestrial laser scanner has been used to identify prone-to-fail configurations in a rock cliff. Rock falls that occurred during 3 years in a limestone cliff have been detected by comparison of successive point clouds. The fallen compartments have been modelled by a mesh using the 3DReshaper software, giving information on volume, dimensions and failure mechanism (slide or topple) of rockfalls. Then the compartments have been approximated by polyhedrons to describe the different failure configurations in relation with the structural settings of the rock mass, which has been studied using the Coltop3D software.

Key words: *Rockfall, Terrestrial laser scanner, LiDAR, Failure configuration.*

1. Introduction

Development of Terrestrial Laser Scanner (TLS) investigation methods help to quantify geological processes, such as rockfalls (ABELLAN *et al*, 2010), erosional processes (LOYE *et al*, 2012, LIM *et al*, 2010), landslides (BRIDEAU *et al*, 2011, OPPIKOFER *et al*, 2009), discontinuity characterisation (STURZENEGGER & STEAD, 2009).This study focuses on an high limestone cliff in the Subalpine ranges, in the French Alps. The TLS investigation permits to get a quasi-exhaustive inventory of rockfalls larger than a threshold for a time period of 3 years. The obtained point clouds were analysed to get a structural analysis at different scales of the cliff, which will be put in relation with the failure configurations (STURZENEGGER *et al*, 2007). It will permit to better estimate the prone-to-fail compartments in relation with the rock mass structure.

2. The Mont Saint Eynard

The Mont Saint Eynard is located North East of Grenoble, Isère, French Alps (figure 1). It is a long doubled cliff, making up the western border of the Isère Valley and the oriental edge of the Chartreuse Massif. It peaks at 1308 m ASL.

Its global morphology consists of two 7 km long subvertical cliffs dipping south-east. The lower cliff is 240m high, separated from the 120m high upper cliff by a ledge covered with forest. This morphology corresponds to a marl-limestone alternation:

- Upper cliff: massive limestone of the Tithonian stage, thickly bedded
- Forested ledge: marl and marly limestone of the lower Kimmeridgian stage
- Lower cliff: thinly bedded limestone of the Sequanian stage (fine calcareous paste with radiolarias, scarce marly beds)
- Talus slope: marls and marly limestones of the Oxfordian stage

The SW-NE trending cliff belongs to the eastern side of the Sappey syncline, which dips North in the direction N10 (figure 1). Two subvertical dextral faults cut the cliff (GIDON, 1990), with a direction of about N60-70. Note that the global direction of the Saint Eynard cliff (N45) is different from the syncline axis (N10).

The whole cliff was surveyed by airborne laser scanning (ALS) in 2011. A first 750m long zone of interest (figure 1) has been yearly surveyed by TLS since 2009. A second 300m long zone if interest, was surveyed by TLS in 2013. This study is focused on the lower cliff because of its higher rockfall activity compared to the upper cliff.

3. Structural analysis by laser scanner

Based on point clouds obtained from airborne and terrestrial laser scanning, the software Coltop3D helped to determine the main discontinuity sets of the rock mass and their orientations.

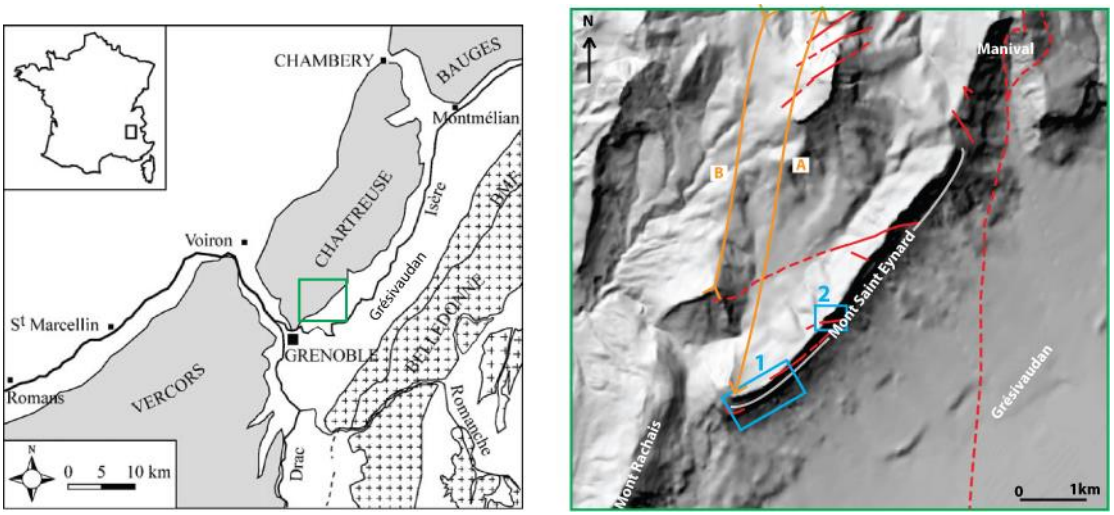

Fig. 1: Left: simplified geological map of the Grenoble area. Shaded: sedimentary massifs; cross pattern: external crystalline massifs; BMF: Belledonne middle fault (after Frayssines, 2006). Right: zoom on the study area; DEM of the Mont St Eynard. A: Sappey syncline, B: Ecoutoux anticline. Continuous and dashed red lines: faults. Blue squares 1 and 2: TLS investigated zones.

Figure 2 shows extracted points from Coltop3D corresponding to the main discontinuity sets. Field measurements were also made in an accessible part of the Mont Saint Eynard. The results are shown in figure 3. The bedding planes orientation varies around the syncline axis. In the Pas de l'Aiguille zone (location 4 in figure 3A), they are roughly parallel to the syncline axis and slightly dipping West. Near the syncline axis, they are dipping North. On the western side of the syncline axis, their dip direction quickly changes to the East, due to the asymmetry of the Sappey syncline. Two directions of subvertical fractures are recurrent: the yellow one, which has a direction of N60, corresponding to the direction of the main faults of the Chartreuse Massif (GIDON, 1990); and the red one, which has a direction of N90.

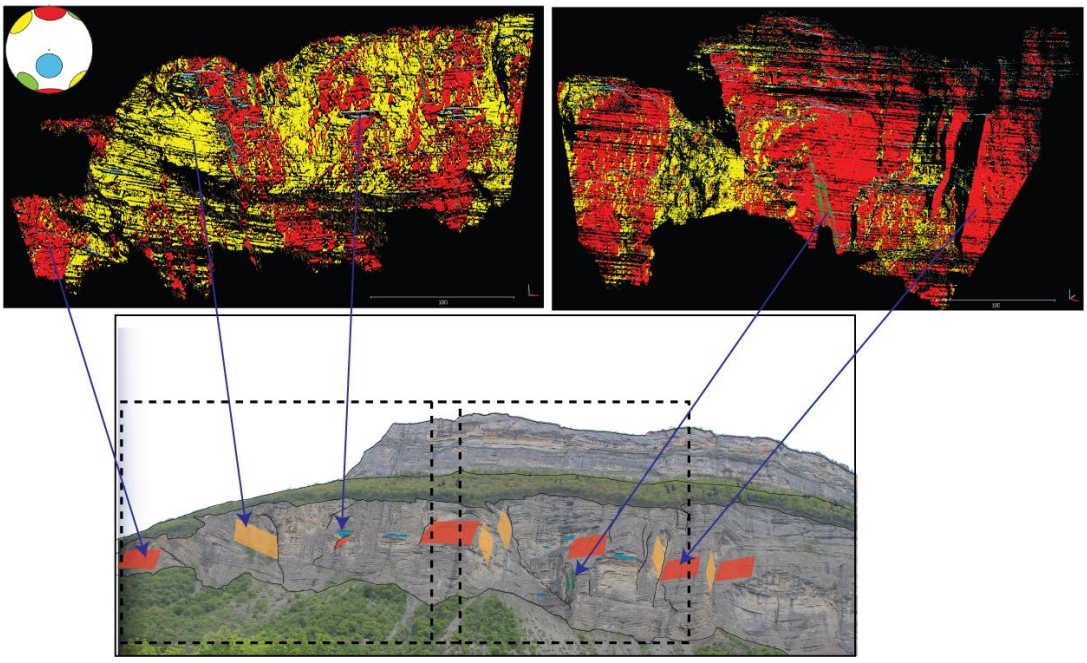

Fig. 2: Up: 2 scenes of Saint Eynard surveyed by TLS, analyzed by Coltop3D. Point clouds were extracted according to the main discontinuity sets defined on the stereographic representation (up left). The ellipses represents pole of discontinuity with variability. Down: photograph of the investigated zone. The dashed line rectangle shows the two scenes of TLS survey. The arrows localize examples of discontinuity planes, colored with respect to the stereographic representation.

The other discontinuity sets are minor, and correspond respectively to the conjugate sets of the yellow set (green) and the red set (brown, figure 3.B). These discontinuity sets are linked to the tectonic history of the Chartreuse Massif (GIDON, 1990).

It can be noticed visually (on the cliff or by horizontal sections, and also on the figure 2) that the cliff is cut at a large scale by two types of fractures which create spurs and recesses. The structural analysis from the ALS (figure 3B) confirmed the observation of the global cutting of the cliff by two sets of discontinuities all along the 7 km of the cliff with spurs and recesses, except locally in the fault zones. A new set appears in the Northern part (locations 4 to 6), quasi parallel to the synclinal axis and dipping East. It can be noticed that this morphology with spurs and recesses is not encountered on the upper cliff of Mont Saint Eynard, which consists of massive limestones.

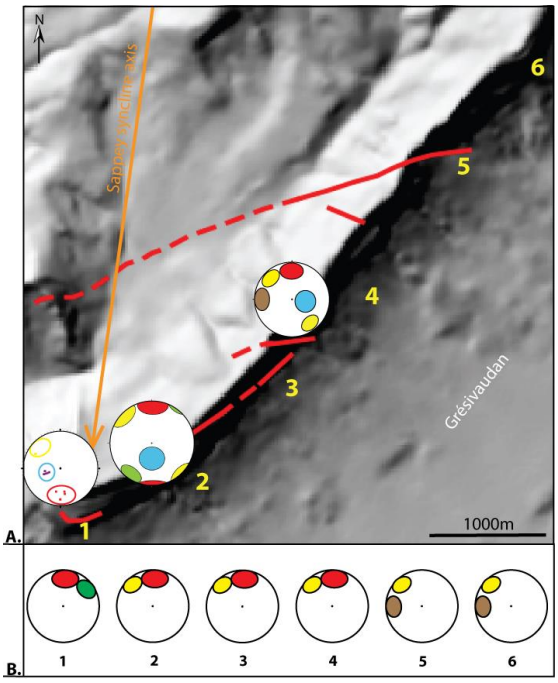

Fig. 3: Evolution of discontinuity sets. A: obtained from local TLS (full ellipses in stereographic projection corresponding to poles of discontinuity with variability) and field measurements (points in empty ellipses). B: main discontinuity sets creating horizontal spurs and recesses, obtained from ALS.

4. Failure configurations

The TLS investigation made since 2009 allowed to detect fallen compartments of volume bigger than 0.01m^3 (GUERIN *et al.*, 2014), using the software 3DReshaper. The volume frequency relation and the 3D reconstruction of these rockfalls are available in GUERIN *et al.* (2014). 162 events were studied, in a volume range of 0.01m^3 to 100m^3. 75% of the rockfall volumes were smaller than 1m^3.

4.1 Configurations of the fallen compartments

The 3D reconstruction based on TLS data gives information on the shape of the fallen compartments, through horizontal and vertical sections. Each compartment has been approximated by a simplified polyhedron of 6 faces, named from A to F according to the figure 6.A. This approximation by a 6 faces polyhedron appears to be close to the real shape of the compartments. The compartments are always cut by two bedding planes. As these planes are slightly inclined, their height has been defined perpendicular to them. The width has been defined parallel to the cliff and the depth perpendicular to it. The height/width average ratio is 0.92, and the height/depth average ratio is 1.56. Figure 4 shows the rockfalls depth and width as a function of height: some points are very dispersed, but most of them are grouped. The fallen compartments are visibly not very deep (less than 10m). Figure 4 also shows the height/depth ratio as a function of height/width. So the typical shape of the fallen compartments can be described as subvertical square slabs.

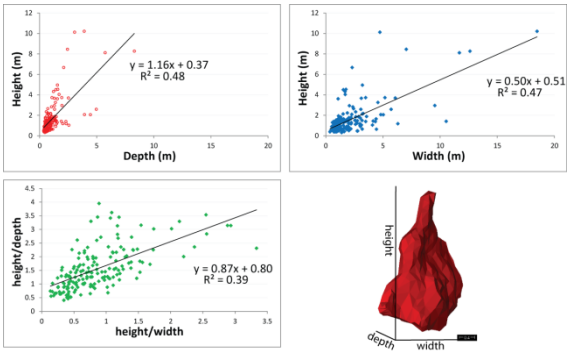

Fig 4: Up: depth (red empty points) and width (blue full points) as a function of height of rockfalls. Down left: height/depth ratio as a function of height/width ratio, for each rockfall. Down right: 3D reconstruction of a fallen compartment and scheme of the 3 considered dimensions.

Each face was defined as a jointed face or not, and also associated to a joint set previously defined (figure 6.B).

Front faces (A) are always free, whereas back faces (C) are always jointed to the cliff (figure 6.B). Both are essentially defined by the F2 discontinuity set. Around 50% of top (D) faces are jointed, and bottom faces (B) are always free. It

means that all rock falls occur in overhang configurations. Top faces and bottom faces are defined by the F1 discontinuity set, i.e. bedding planes. Lateral left (E) and right (F) faces are sometimes jointed (around 15%) and defined respectively by F3 and F4 discontinuity set, but these faces could not always be easily determined.

Fallen compartments are essentially cut by bedding planes and sub vertical discontinuities of directions N90, creating overhangs. According to FRAYSSINES ET AL. (2006), the back face of fallen compartments (C) in this type of limestone cliff is mainly defined by a pre-existing joint. Considering the lower cliff of Saint Eynard, in half of the failure cases, the joint defining the back face (C) stops on a new overhang, on which a new rockfall can occur, until it reaches the top end of the cliff. It would tend to form an equilibrium profile, for example of a uniform slope, which would also tend to minimize the rockfall hazard at long term. But new overhanging is created in foot of the cliff due to the erosion of the underlying marls. This has still to be quantified. Some small parts of the cliff already present a uniform slope and a smoothed surface (figure 5): there is no overhang and the limestone beds are very slightly marked. In these very localized zones, none or a few rockfalls occurred.

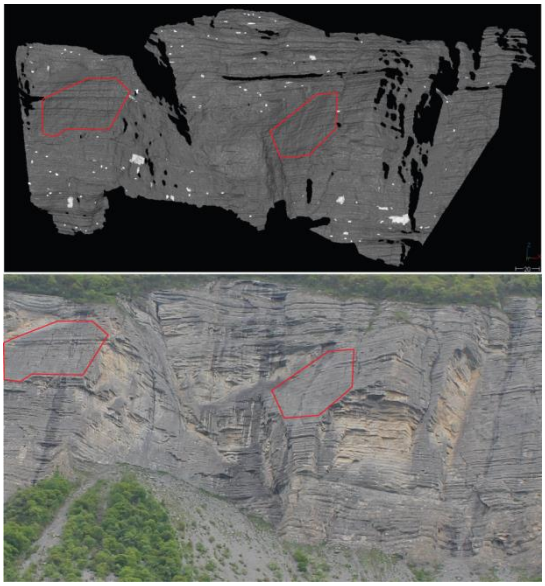

Fig. 5: Up: 3D view of the left TLS surveyed scene. White points are detected rockfalls. Down: photograph of the left scene, location of smoothed surfaces with no rockfalls.

The link between cliff roughness and rockfall frequency will be studied later starting from these observations, which are made all along the 7km of cliff.

4.2 Failure mechanisms

The compartment volume and its gravity center are known by 3D reconstruction (figure 6.C). The weight vector has been built starting from the gravity center. Considering that the only moving force is gravity, information on failure mechanisms could be obtained. Two main types of failure were considered: slide and topple. They request different mechanical properties of the discontinuity (figure 6.C). When the half line of weight intersects a jointed face of the compartment, the mechanism is a slide. When it intersects a free face, topple and more rarely free fall were possible and the intersected free face was overhanging. Topple and free fall were not distinguished because it was not possible to know where the rock bridges were and it did not permit to know the real fall movement.

The topple mechanism is largely dominant (more than 80%), emphasised by the configurations of the compartments, which are overhanging, and the global cliff morphology: discontinuities are sub horizontal (bedding planes) and sub vertical (fracturing). This doesn't create lots of sliding planes.

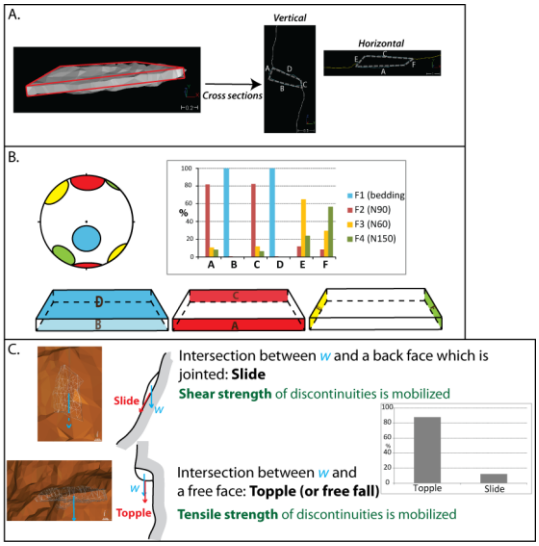

Fig. 6: A: scheme of the 6 faces approximation; B: distribution of directions of the faces; C: examples and schemes of the failure mechanisms, and proportions of failure mechanisms.

5. Conclusion

The rock mass structure has been studied from laser scanner data completed with field measurements. The results are consistent with the structural context of the Sappey syncline and the Chartreuse Massif. The cliff surface is defined essentially by the main discontinuity sets: subvertical

fractures and bedding planes making up overhangs.

The failure configurations and mechanisms have been studied by comparing successive TLS point clouds. In the Mont Saint Eynard thinly bedded limestone cliff, the prone-to-fall configurations are overhangs and the main failure mechanism is topple. Typical fallen compartments can be described as subvertical square slabs.

Acknowledgements: The authors would like to thank the PARN (Pole Alpin Risques Naturels) for providing the ALS data of the Saint Eynard cliff. Funding for this project was provided by a grant from La Région Rhône-Alpes.

References

ABELLAN, A., CALVET J., VILAPLANA J-M. & BLANCHARD J. (2012): *Detection and spatial prediction of rockfalls by means of terrestrial laser scanner monitoring.* Geomorphology, 119, 162-171.

BRIDEAU, MA., PEDRAZZINI, A, STEAD, D., FROESE C., JABOYEDOFF, M. & VAN ZEYL, D. (2011) : *Three-dimensional slope stability analysis of South Peak, Crowsnest Pass, Alberta, Canada*. Landslides, 8, 139-158.

FRAYSSINES, M. & HANTZ, D. (2006): *Failure mechanisms and triggering factors in calcareous cliffs of the Subalpine Ranges (French Alps)*. Engineering Geology, 86, 256-270.

GIDON, M. (1990) : *Les décrochements et leur place dans la structuration du massif de la Chartreuse (Alpes occidentales françaises).* Géologie Alpine, 66.

GUERIN, A., ROSSETTI, JP., HANTZ D. & JABOYEDOFF M. (2014) : Brief communication : *Estimating rockfall frequency in a mountain limestone cliff using terrestrial laser scanner*. Nat. Hazards Earth Syst. Sci. Discuss., 2, 123-135.

LIM, M., ROSSER, N.J., ALLISON, R.J. & PETLEY, D.N. (2010): *Erosional processes in the hard rock coastal cliffs at Staithes, North Yorkshire.* Geomorphology, 114, 12-21.

LOYE, A., PEDRAZZINI A., THEULE, JI, JABOYEDOFF, M., LIÉBAULT F. & METZGER, R. (2012): *Influence of bedrock structures on the spatial pattern of erosional landforms in small alpine catchments*. Earth Surf. Process. Landforms, 37 (13), 1407-1423.

OPPIKOFER, T., JABOYEDOFF, M., BLIKRA. L, DERRON, M-H & METZGER, R. (2009): *Characterisation and monitoring of the Aknes rockslide using terrestrial laser scanning*. Nat. Hazards Earth Syst. Sci, 9, 1003-1019.

STURZENEGGER, M., SARTORI, M., JABOYEDOFF, M. & STEAD, D. (2007): *Regional deterministic characterization of fracture networks and its application to GIS-based rockfall risk assessment*. Engineering Geology, 94, 201-214.

STURZENEGGER, M. & STEAD, D. (2009): *Close-range terrestrial digital photogrammetry and terrestrial laser scanning for discontinuity characterization on rock cuts*. Engineering Geology, 106, 163-182.